

Bayesian neural network with pretrained protein embedding enhances prediction accuracy of drug-protein interaction

QHwan Kim¹, Joon-Hyuk Ko¹, Sunghoon Kim¹, Nojun Park¹, and Wonho Jhe^{1*}

¹Department of Physics and Astronomy, Institute of Applied Physics, Seoul National University, Gwanak-gu, Seoul 08826, Republic of Korea.

*whjhe@snu.ac.kr

ABSTRACT

The characterization of drug-protein interactions is crucial in the high-throughput screening for drug discovery. The deep learning-based approaches have attracted attention because they can predict drug-protein interactions without trial-and-error by humans. However, because data labeling requires significant resources, the available protein data size is relatively small, which consequently decreases model performance. Here we propose two methods to construct a deep learning framework that exhibits superior performance with a small labeled dataset. At first, we use transfer learning in encoding protein sequences with a pretrained model, which trains general sequence representations in an unsupervised manner. Second, we use a Bayesian neural network to make a robust model by estimating the data uncertainty. As a result, our model performs better than the previous baselines for predicting drug-protein interactions. We also show that the quantified uncertainty from the Bayesian inference is related to the confidence and can be used for screening DPI data points.

Identifying novel drug-protein interactions (DPIs) have been studied broadly for predicting potential side effects¹, toxicities², and repositioning of drugs^{3,4}. However, quantification of DPI of every possible drug-protein pair is prohibitively time-consuming and expensive since it requires individual experiments or simulations for each pair.

With the development of protein sequence and drug-protein interaction public datasets^{5,6},

machine learning-based methods^{7–10} have emerged as candidate of fast DPI identification. Recently, deep neural networks (DNNs) have attracted attention because they outperform other machine learning-based methods in various tasks, such as computer vision¹¹ and natural language processing^{12,13}.

In the usual DPI task, a protein is represented as a 1-dimensional long sequence of amino acid characters. Thus the deep learning models for natural language processing have been broadly used to obtain useful protein features from the sequences. Previous studies in this approach include using recurrent neural networks with long short-term memory (LSTM)¹⁴ or gated recurrent unit (GRU)¹⁵ layers for their ability to identify long-term dependencies in sequential data^{16–18}. The other studies have used convolutional neural networks (CNN)^{19–23} to extract hidden local patterns in sequences. Different representations of proteins, such as 2-dimensional contact maps^{24,25} or 3-dimensional atom coordinates^{26,27}, in addition to 1-dimensional sequences, also have been used to increase model performance.

Supervised training of high-capacity DNN models from scratch requires a large amount of labeled training data points. For example, Mahajan *et al.*²⁸ showed that the more labeled data is required to increase accuracy after training with 10^9 images. However, currently available DPI datasets usually contain thousands of labeled protein sequences, a small number compared to the > 195 M unrevealed interaction information in UniProtKB²⁹. The lack of qualified labeled data points suppresses the usage of more elaborated deep learning architectures, which could potentially increase performance and reliability³⁰. In particular, the scarcity of labeled data of biology and chemistry-related tasks has been suggested consistently^{10,31} although the labeling require expensive and time-consuming experiments.

To overcome the difficulties of learning with limited data, several studies have proposed methods to increase the expressiveness of the deep learning model without additional endeavor to label generation. Of those, transfer learning uses a model that is initially pretrained with a large corpus of data of different task. This pretrained model is then transferred to the target tasks by adding classification layers and fine-tuning with the original small dataset. Transfer learning approaches have shown substantial performance improvement in computer vision³²,

natural language processing¹³, and structure-property prediction of molecules^{33,34}. In cases where labeled data is expensive, such as in scientific problems, the pretrained model can be prepared in an unsupervised manner, using large but unlabeled datasets. Winter et al.³³ trained an autoencoder model with a huge corpus of chemical structures and used them to predict molecular properties. Villegas-Morcillo *et al.*³⁵ showed that the supervised classification tasks with a pretrained protein sequence model could achieve competitive performance with other complicated models.

Another proposed method to obtain a more robust and reliable model with a small dataset is Bayesian neural network (BNN)³⁶. Compared to a conventional DNN, which gives definite point prediction for each given input, a BNN returns a distribution of predictions, which qualitatively corresponds to the aggregate prediction of an ensemble of different neural networks trained on the same dataset. Direct implementation of BNN is infeasible because training an ensemble of neural networks requires enormous computing power. Monte-Carlo dropout (MC-dropout) approach^{37,38} enables reasonable training time of BNNs by approximating the posterior distribution of network weights by a product of the Bernoulli distribution with dropout layers.

Here, we propose an end-to-end deep learning framework for highly accurate DPI prediction with transfer learning and BNN. We choose the pretrained model as a stacked transformer architecture, which is trained with 250 million unlabelled protein sequences in an unsupervised manner³⁹. The drug is represented by the molecular graph and encoded through the graph interaction network layers. Estimation of the model performance using three public DPI datasets shows that the proposed model outperforms previous approaches. In addition, the estimated uncertainty, which is obtained from the sampling output of BNN, is decomposed into model-based and data-based elements, which can be used to further virtual screening of data points. In summary, the main contributions of our work are as follows.

1. We propose the first approach to predict DPI with the Bayesian neural network framework and the pretrained protein sequence model;
2. our method demonstrates highly accurate prediction of three public DPI datasets;

3. the output of BNN can estimate the confidence of the data points.

Experiments

Datasets

We evaluate our model and other baseline models on three public DPI datasets: the BindingDB dataset¹⁶, the Human dataset⁶, and the *C. elegans* dataset⁶.

BindingDB

BindingDB is a public database of experimentally measured binding affinities between the small molecules and proteins⁵. The original dataset contains 1.3 million interaction labels with quantitative measurements of IC₅₀, EC50, and Ki. We use the binarized version of BindingDB dataset constructed by Gao *et al.*¹⁶, which contains 39,747 positive interactions and 31,218 negative interactions. The training/validation/testing split is prepared in the dataset. The training set contains 28,240 positive and 21,915 negative interactions. The validation set contains 2,831 positive and 2,776 negative interactions. And the test set contains 2,706 positive and 2,802 negative interactions.

Human and C. elegans

Created by Liu *et al.*⁶, these datasets include highly credible negative samples of compound-protein pairs obtained by using a systematic screening framework. Following Tsubaki *et al.*²², we use the balanced and the unbalanced dataset, where the ratios of the positive to negative samples are 1:1 and 1:3, respectively. The human dataset contains 3,369 positive interactions between 1,052 unique drugs and 852 unique proteins; the *C. elegans* dataset contains 4,000 positive interactions between 1,434 unique drugs and 2,504 unique proteins. Also, we use an 80%/10%/10% training/validation/testing random split.

Proposed Model

In this study, the DPI is defined as a binary label, which represents the presence of an interaction. Figure 1 (a) shows schematic of proposed model. The input data is a pair of strings

consisting of a protein sequence and drug SMILES strings. The input data passes embedding layers to be encoded as a pair of representation vectors. These protein and drug representation vectors are then concatenated and passed through fully-connected layers, resulting in a prediction for the existence of an interaction. In each cycle of training, this prediction is compared with the ground truth, and model parameters are tuned to decrease the difference between the two using the backpropagation algorithm. To implement BNNs, we apply dropout layers in every layer except the pretrained layer, the concatenation layer, and the final fully-connected layer. Detailed descriptions of the model are given below.

Feature extraction of protein

A protein sequence is represented as a list of amino acids provided in the raw training data. Note that we do not use a set of gene ontology annotations that provides high-level information on protein functions. To extract protein-level embeddings, we use the pretrained models from Rives *et al.*³⁹, which were trained with 250 million protein sequences in an unsupervised manner. Rives *et al.* used an attention-based transformer architecture¹², and found that their model outperforms other recurrent network-based methods for predicting protein functionality. We select three models, Trans6, Trans12, and Trans34, which are pretrained with 6, 12, and 34 transformer layers, respectively.

For each protein sequence of length L_p , the pretrained models outputs an embedding matrix $\mathbf{X}_p \in \mathbb{R}^{L \times d}$, where $d = 768$ for Trans6, Trans12 and $d = 1,280$ for Trans34 model. From amino-acid level feature \mathbf{X}_p , we obtain the protein level feature $\mathbf{x}_p^{(0)} \in \mathbb{R}^d$ by averaging over the L amino acids features.

With the protein-level embedding $\mathbf{x}_p^{(0)}$, we use three 1-dimensional convolutional neural networks (1D-CNN) to smooth patterns in protein features. Note that the 1D-CNN gives slightly better performance than the fully-connected layers.

Feature extraction of drug

The raw training data of drugs is in the SMILES (Simplified Molecular Input Line Entry System) format⁴⁰. For each input SMILES string, we construct a corresponding molecular graph that

contains connectivity and structure information of the compound.

In the molecular graph, atoms and bonds are represented with vectors with structural features that characterize the surrounding chemical environment. The details of the attributes are shown in Supplementary Table 1, which follows the feature design from DeepChem⁴¹. The graph construction and corresponding feature extraction processes are conducted using RDKit⁴² - an open-source chemical informatics software. Initial encoding of the i -th atom and bond between the i - and j -th atoms are denoted as vectors, $\mathbf{v}_i^{(0)}$ and $\mathbf{e}_{ij}^{(0)}$, respectively. These atom and bond features are updated by a message passing-based graph network during model inference.

The message passing framework of graph data has been used broadly to predict the properties of crystal⁴³, organic molecules³¹, ice⁴⁴, and glasses⁴⁵. To extract the drug molecule features, we use the graph interaction network (GraphNet) model⁴⁶. Figure 1 (b) shows the schematic of the GraphNet mechanism. First proposed by Battaglia *et al.*⁴⁶ to infer interaction between objects, the GraphNet exchanges information between graph edges and nodes and recursively updates them.

The GraphNet first updates an edge between i - and j -th node as,

$$\mathbf{e}_i^{(l+1)} = \text{ReLU} \left[\left(\mathbf{e}_{ij}^{(l)} \oplus \mathbf{v}_i^{(l)} \oplus \mathbf{v}_j^{(l)} \right) \mathbf{W}_e^{(l)} + \mathbf{b}_e^{(l)} \right], \quad (1)$$

where \oplus is the concatenation operator, $\mathbf{W}_e^{(l)}$ is the weight matrix of the edge update, and $\mathbf{b}_e^{(l)}$ is the bias. Then update of the i -th node is carried out with the features of the node and on the sum of its linked edge features as,

$$\mathbf{v}_i^{(l+1)} = \text{ReLU} \left[\left(\mathbf{v}_i^{(l)} \oplus \sum_{j \in N(i)} \mathbf{e}_{ij}^{(l+1)} \right) \mathbf{W}_v^{(l)} + \mathbf{b}_v^{(l)} \right], \quad (2)$$

where $\mathbf{W}_v^{(l)}$ is the weight matrix of node update, and $\mathbf{b}_v^{(l)}$ is the bias. After the update of node states is finalized, we obtain a graph feature (molecular feature) by gathering all the node and edge states. We choose most typical readout function, which is an average of all atom states

processed by,

$$\mathbf{x}_d = \frac{1}{N} \sum_i (\mathbf{v}_i \oplus \mathbf{e}_i), \quad (3)$$

where N is the number of nodes in the molecular graph.

Classifier

We prepare the drug-protein feature vector \mathbf{x} by concatenating \mathbf{x}_p and \mathbf{x}_d ,

$$\mathbf{x} = \mathbf{x}_p \oplus \mathbf{x}_d. \quad (4)$$

In the classifier block, the feature vector \mathbf{x} passes fully connected (FC) layers with ReLU activation to output final prediction value. The dimension of the last layer is 2, corresponding to the one-hot encoding of the binary classification labels.

Bayesian neural network

For a given training set $\{\mathbf{X}, \mathbf{Y}\}$, let $p(\mathbf{Y}|\mathbf{X}, \mathbf{w})$ and $p(\mathbf{w})$ be model likelihood and prior distribution for a vector of model parameters $\mathbf{w} \in \Omega$, respectively. In a Bayesian framework, model parameters and the output are considered as random variables. The predictive distribution is defined as

$$p(\mathbf{y}^*|\mathbf{x}^*, \mathbf{X}, \mathbf{Y}) = \int_{\Omega} p(\mathbf{y}^*|\mathbf{x}^*, \mathbf{w}) p(\mathbf{w}|\mathbf{X}, \mathbf{Y}) d\mathbf{w} \quad (5)$$

for a new input \mathbf{x}^* and a new output \mathbf{y}^* . In a neural network with classification tasks, the predictive probability is given by the neural network output which is passed through a final softmax activation function.

The direct computation of Eq. (5) in DNN is often infeasible because the integration over the parameter space requires heavy computational costs. Many practical methods have been proposed to approximate the posterior and carry out the integration via sampling technique. A variational inference approximates the posterior distribution with a tractable distribution $p(\mathbf{w}|\mathbf{X}, \mathbf{Y}) \sim$

$q_\theta(\mathbf{w})$ parameterized by a variational parameter θ . The quality of variational distribution $q_\theta(\mathbf{w})$ is crucial to the implementation of BNN. The recently proposed Monte-Carlo dropout (MC-dropout) approach uses a dropout variational distribution to approximate the posterior distribution with a product of Bernoulli distributions³⁷. The MC-dropout method is practical because it does not need extra learnable parameters to model the variational posterior distribution and the integration over the whole parameter space can be easily approximated with the collection of outputs sampled by repeated inference of text input \mathbf{x}^* while the dropout layers are turned on. Thus, we adopt MC-dropout in this work.

A variational inference approximating a posterior a variational distribution $q_\theta(\mathbf{w})$ provides a variational predictive distribution of a new output \mathbf{y}^* given a new input \mathbf{x}^* as

$$q_\theta^*(\mathbf{y}^*|\mathbf{x}^*) = \int_{\Omega} q_\theta(\mathbf{w}) p(\mathbf{y}^*|f^{\mathbf{w}}(\mathbf{x}^*)) d\mathbf{w}, \quad (6)$$

where $f^{\mathbf{w}}(\mathbf{x}^*)$ is a model output with a given \mathbf{w} . For classification tasks in BNN, the integration in Eq. (6) is replaced with a predictive mean of T times of MC sampling, which is estimated by

$$\hat{E}[\mathbf{y}^*|\mathbf{x}^*] = \frac{1}{T} \sum_{t=1}^T f^{\hat{\mathbf{w}}_t}(\mathbf{x}^*) = \frac{1}{T} \sum_{t=1}^T \hat{\mathbf{y}}_t^*. \quad (7)$$

In estimating its predictive variance, we decompose the source of uncertainty into aleatoric and epistemic, which was first suggested by Kendall and Gal³⁸ and optimized for classification tasks by Kwon *et al.*⁴⁷. The aleatoric uncertainty originates from the inherent noise of data points, and the epistemic uncertainty arises due to model prediction variability. Here we use the method suggested by Kwon *et al.*⁴⁷, which does not involve extra parameters.

The predictive variance is estimated by

$$\hat{\text{Var}}[\mathbf{y}^*|\mathbf{x}^*] = \underbrace{\frac{1}{T} \sum_{t=1}^T (\hat{\mathbf{y}}_t^* - \bar{\mathbf{y}})(\hat{\mathbf{y}}_t^* - \bar{\mathbf{y}})^T}_{\text{epistemic}} + \underbrace{\frac{1}{T} \sum_{t=1}^T \left(\text{diag}(\hat{\mathbf{y}}_t^*) - (\hat{\mathbf{y}}_t^*)(\hat{\mathbf{y}}_t^*)^T \right)}_{\text{aleatoric}}, \quad (8)$$

where $\bar{\mathbf{y}} = \sum_{t=1}^T \hat{\mathbf{y}}_t^*/T$ and $\hat{\mathbf{y}}_t^* = \text{softmax}(\mathbf{f}^{\hat{\mathbf{w}}_t}(\mathbf{x}^*))$.

Implementation and Evaluation Strategy

We implement the proposed model with Pytorch 1.5.1⁴⁸. The training process takes at most 200 epochs on all the datasets using the Adam optimizer⁴⁹ with a learning rate of 0.001 and a batch size of 32. The hidden layer dimensions of GraphNet in the drug feature extractor and MLP in the classifier are 256 and 512, respectively. The number of layers of both the protein and drug feature extractor is set to 3. The coefficient of L2 regularization is 0.001. These hyperparameters are searched in a wide range.

The training objective is to minimize the loss function \mathcal{L} , given by the sum of the cross-entropy loss and the regularization as follows

$$\mathcal{L}(\mathbf{w}) = - \sum_{i=1}^N y_i [\log \hat{y}_i + (1 - y_i) \log (1 - \hat{y}_i)] + \frac{\lambda}{2} \|\mathbf{w}\|_2^2, \quad (9)$$

where \mathbf{w} is the set of model parameters, N is the number of interaction labels, and λ is an L2 regularization hyperparameter.

To implement MC-dropout sampling, we turn on dropout layers in estimating test dataset with $T = 30$ samplings. The mean performance and the decomposed uncertainties of the output are calculated with Eq. (7) and Eq. (8), respectively.

The main performance metric was chosen to be the area under the receiver operating curve (ROC-AUC). We also report some additional performance metrics - accuracy for the BindingDB dataset, and precision and recall for the Human and *C. elegans* dataset.

Results

To train DPI datasets, we prepare six models, Trans6, Trans12, Trans34, Trans6+Drop, Trans12+Drop, and Trans34+Drop. The latter three models use the pretrained protein model and implement the BNN architecture with MC-Dropout (Fig. 1 (a)), while the former three models only use the pretrained model. The numbers 6, 12, and 34 correspond to the number of transformer layers in the pretrained model.

Performance of proposed model

With the BindingDB dataset, we compare our model against three baselines: Tiresias, DBN, and E2E. Tiresias uses similarity measures of drug and protein pairs⁷. DBN uses stacked restricted Boltzmann machines with the inputs as extended connectivity fingerprints⁹. E2E uses graph convolutional networks and LSTM to process drug-protein pair information with Gene Ontology annotations¹⁶.

Following suggestions from previous works, we further split the test dataset into four sub-test sets that the model can be learned and applied to predict the label between a drug and protein target. The binary interaction test data is divided by “seen” and “unseen” whether the protein and drug are observed in the training dataset.

Figure 2 shows that the proposed method consistently performs well on all four sub-test sets. The models with pretraining and MC-dropout give a high performance consistently in four categories. The sub-test dataset with unseen protein is difficult to classify, while only the E2E model shows comparable performance with our proposed model. Tiresias and DBN perform well on seen proteins and outperform E2E but have much worse performance on unseen proteins because these models are overfitted. The score of the unseen protein dataset is consistently lower than that of the unseen drug dataset. It implies that the extraction of generalized protein embedding with a long sequence plays an important role in DPI classification. If we measure scores with aggregating four test sub-datasets, the ROC-AUC of Trans6+Drop, which achieves the best score in the proposed model, is 0.943 while that of E2E is 0.913 and DBN is 0.817.

Also, we compare the proposed method with the previous DPI approaches on the Human and the *C. elegans* dataset. We compare it with k-nearest neighbor (k-NN), random forest (RF), L2-logistic (L2), support vector machine (SVM), and graph neural network (GNN) models. Note that the GNN model uses *n*-grams to embed protein sequence.

As shown in Tables 1, the our best performing model achieves the highest AUC, precision, and recall scores among the neural network-based method. In the human dataset, SVM shows better performance in the Precision score, but the proposed model outperforms the other metrics. In the *C. elegans* dataset, Trans6+Drop shows the best performance all metrics, except

the recall score of the balanced dataset that Trans34+Drop is the best.

Our results show that models with both transfer learning and BNN (Trans6+Drop, Trans12+Drop, Trans34+Drop) outperform other baseline models when evaluated with three public DPI datasets. We note that only the pretrained protein sequence can train models (Trans6, Trans12, Trans34) competitive with the baselines, but additional Bayesian frameworks further increase performance. It suggests that the role of BNN, training robust model, is the key figure of performance enhancement as well as the expression capacity obtained from the pretrained model.

An additional point to mention is that the most complex model, Trans34+Drop, does not always give the best results. This is in agreement with the literature, where it was found that the prediction accuracy is not strictly proportional to the sequence model complexity³⁹. Therefore, when using transfer learning, we recommend preparing several different pretrained models and comparing their results before making the final choice.

Robustness of proposed model

In this section, we test the robustness of the Bayesian models by varying the quality of the protein data. The robustness is estimated by tracking the degradation of the model performance as more and more external noise is added to the dataset. The type of noise for the experiment is chosen to be the Gaussian noise $\mathcal{N}(0, \sigma^2)$, where 0 is the mean and σ is the standard deviation of the distribution.

Figure 3 shows the ROC-AUC scores of the two models Trans6 and Trans6+Drop applied to three DPI datasets as a function of the noise level σ . As the noise level increases, the ROC-AUC of Trans6+Drop is more robust to the additive noise than that of Trans6. In the BindingDB dataset, the ROC-AUC score of Bayesian Trans6+Drop does not fall under 0.8 when noise standard deviation increases until 0.5, where Trans6 loses its predictability. For Human and *C. Elegans* datasets, the models maintain relatively good performance regardless of the additive noise, where the Bayesian model outperforms the other. It indicates that the BNN architecture trains more robust model and it attributes the overall enhanced performance of our proposed model.

Quality of estimated uncertainties

We first test whether the uncertainties obtained from the proposed BNN model are correctly estimated. This is accomplished by reducing the training set sizes and observing the resulting uncertainty changes. When dataset size is decreased, aleatoric uncertainty, which is related to the inherent noise of the data, should stay constant, whereas the model error-related epistemic noise should increase to a lack of sufficient training data.

Table 2 shows the uncertainties obtained from the reduced training set sizes (1, 1/2, 1/4) and the entire test set. The uncertainties are obtained via Eq. (8). It shows that the epistemic uncertainty increases as the training size gets larger, while the aleatoric uncertainty remains relatively constant. It indicates that our proposed model reliably estimate uncertainties.

Because the model successfully estimates uncertainties, we can plot confidence-accuracy graphs, as shown in Fig. 4. We use three uncertainties, an epistemic uncertainty, aleatoric uncertainty, and the sum of two. Here the confidence percentile means that we only consider the top n percent of data points in the test set ranked by the confidence, which is defined by the inverse of uncertainty. The plots show how the test set accuracy varies as a function of the confidence percentile. In every dataset, the accuracy is an increasing function of model confidence. Thus the data points with low confidence can be interpreted as the outlier and can be screened in DPI datasets in drug development applications. For example, if we delete 50 % of the lowest confident points of the Human dataset, we can achieve nearly 100 % accuracy. Note that there is no consistent trend regarding which uncertainty is more important, and two uncertainties should be treated equally to achieve an accurate estimation.

Conclusion

In this study, we present a novel Bayesian deep learning framework with a pretrained protein sequence model to predict drug-protein interactions. Experiments on three public datasets demonstrate that our proposed model consistently outputs increased prediction accuracies. Our estimation of model performance shows that Bayesian neural networks are highly robust to additive

noise, which explains the superior performances of the proposed model. Furthermore, from the prediction uncertainty our model outputs, one can evaluate the confidence level of a dataset, which can then be used to screen the dataset for unreliable data points.

Code availability

The code is available in <https://github.com/QHwan/PretrainDPI>.

References

1. Mizutani, S., Pauwels, E., Stoven, V., Goto, S. & Yamanishi, Y. Relating drug-protein interaction network with drug side effects. *Bioinformatics* **28**, i522–i528 (2012).
2. Liebler, D. C. & Guengerich, F. P. Elucidating mechanisms of drug-induced toxicity. *Nat. Rev. Drug Discov.* **4**, 410–420 (2005).
3. Pushpakom, S. *et al.* Drug repurposing: progress, challenges and recommendations. *Nat. Rev. Drug Discov.* **18**, 41–58 (2019).
4. Xue, H., Xie, H. & Wang, Y. Review of drug repositioning approached and resources. *Int. J. Biol. Sci.* **14**, 1232–1244 (2018).
5. Liu, T., Lin, Y., Wen, X., Jorissen, R. N. & Gilson, M. K. BindingDB: a web-accessible database of experimentally determined protein-ligand binding affinities. *Nucleic Acids Res.* **35**, D198–D201 (2007).
6. Liu, H., Sun, J., Guan, J., Zheng, J. & Zhou, S. Improving compound-protein interaction prediction by building up highly credible negative samples. *Bioinformatics* **31**, i221–i229 (2015).
7. Fokoue, A., Sadoghi, M., Hassanzadeh, O. & Zhang, P. Predicting drug-drug interactions through large-scale similarity-based link prediction. *Int. Semantic Web Conf.* 774–789 (2016).

8. He, T., Heidemeyer, M., Ban, F., Cherkasov, A. & Ester, M. SimBoost: a read-across approach for predicting drug-target binding affinities using gradient boosting machines. *J. Cheminformatics* **9**, 24 (2017).
9. Wen, M. *et al.* Deep-learning-based drug-target interaction prediction. *J. Proteome Res.* **16**, 1401–1409 (2017).
10. Vamathevan, J. *et al.* Applications of machine learning in drug discovery and development. *Nat. Rev. Drug Discov.* **18**, 463–477 (2019).
11. He, K., Zhang, X., Ren, S. & Sun, J. Deep residual learning for image recognition. *Proc. IEEE Conf. on Comput. Vis. Pattern Recognit. (CVPR)* 1017–1024 (2015).
12. Vaswani, A. *et al.* Attention is all you need. *Adv. Neural Inf. Process. Syst.* **301** (2017).
13. Devlin, J., Chang, M.-W., Lee, K. & Toutanova, K. BERT: Pre-training of deep bidirectional transformers for language understanding. Preprint at <http://arxiv.org/abs/1810.04085> (2019).
14. Hochreiter, S. & Schmidhuber, J. Long short-term memory. *Neural Comput.* **9**, 1735–1780 (1997).
15. Cho, K., van Merriënboer, B., Bahdanau, C. & Bengio, Y. On the properties of neural machine translation: Encoder-decoder approaches. *Proc. SSST-8, Eighth Work. on Syntax, Semant. Struct. Stat. Transl.* 103–111 (2014).
16. Gao, K. Y. *et al.* Interpretable drug target prediction using deep neural representation. *Proceeding sof Twenty-Seventh Int. Jt. Conf. on Artif. Intell. (IJCAI-18)* (2018).
17. Karimi, M., Wu, D., Wang, Z. & Shen, Y. DeepAffinity: interpretable deep learning of compound-protein affinity through unified recurrent and convolutional neural networks. *Bioinformatics* **35**, 3329–3338 (2019).
18. Wang, Y.-B. *et al.* A deep learning-based method for drug-target interaction prediction based on long short-term memory neural network. *BMC Med. Inform. Decis. Mak.* **20**, 49 (2020).

19. Öztürk, H., Özgür, A. & Ozkirimli, E. DeepDTA: deep drug-target binding affinity prediction. *Bioinformatics* **34**, i821–i829 (2018).

20. Lee, I., Keum, J. & Nam, H. DeepConv-DTI: Prediction of drug-target interactions via deep learning with convolution on protein sequences. *PLoS Comput. Biol.* **15**, e1007129 (2019).

21. Shin, B., Park, S., Kang, K. & Ho, J. C. Self-attention based molecule representation for predicting drug-target interaction. *Proc. Mach. Learn. Res.* **106**, 230–248 (2019).

22. Tsubaki, M., Tomii, K. & Sese, J. Compound-protein interaction prediction with end-to-end learning of neural networks for graphs and sequences. *Bioinformatics* **35**, 309–318 (2019).

23. Zhang, H., Liao, L., Saravana, K. M., Yun, P. & Wei, Y. DeepBindRG: a deep learning based method for estimating effective protein-ligand affinity. *PeerJ* **7**, e7362 (2019).

24. Jiang, M. *et al.* Drug-target affinity prediction using graph neural network and contact maps. *RSC Adv.* **10**, 20701–20712 (2020).

25. Zheng, S., Li, Y., Chen, S., Xu, J. & Yang, Y. Predicting drug protein interaction using quasi-visual question answering system. *Nat. Mach. Intell.* **2**, 134–140 (2020).

26. Lim, J. *et al.* Predicting drug-target interaction using a novel graph neural network with 3d structure-embedded graph representation. *J. Chem. Inf. Model.* **59**, 3981–3988 (2019).

27. Morrone, J. A., Weber, J. K., Huynh, T., Luo, H. & Cornell, W. D. Combining docking pose rank and structure with deep learning improves protein-ligand binding mode prediction over a baseline docking approach. *J. Chem. Inf. Model.* **60**, 4170–4179 (2020).

28. Mahajan, D. *et al.* Exploring the limits of weakly supervised pretraining. Preprint at <https://arxiv.org/abs/1805.00932> (2018).

29. Consortium, T. U. UniProt: a hub for protein information. *Nucleic Acids Res.* **43**, D204–D212 (2015).

30. Brigato, L. & Iocchi, L. A close look at deep learning with small data. Preprint at <https://arxiv.org/abs/2003.12843> (2020).

31. Ryu, S., Kwon, Y. & Kim, W. Y. A Bayesian graph convolutional network for reliable prediction of molecular properties with uncertainty quantification. *Chem. Sci.* **10**, 8438–8446 (2019).
32. Kornblith, S., Shlens, J. & Le, Q. V. Do better imagenet models transfer better? Preprint at <https://arxiv.org/abs/1805.08974> (2019).
33. Winter, R., Montanari, F., Noé, F. & Clevert, D.-A. Learning continuous and data-driven molecular descriptors by translating equivalent chemical representations. *Chem. Sci.* **10**, 1692–1701 (2019).
34. Hu, W. *et al.* Strategies for pre-training graph neural networks. Preprint at <https://arxiv.org/abs/1905.12265> (2019).
35. Villegas-Morcillo, A. *et al.* Unsupervised protein embeddings outperform hand-crafted sequence and structure features at predicting molecular function. *Bioinformatics* btaa701 (2020).
36. Gal, Y. & Ghahramani, Z. Bayesian convolutional neural networks with bernoulli approximate variational inference. Preprint at <https://arxiv.org/abs/1506.02158> (2015).
37. Gal, Y. & Ghahramani, Z. Dropout as a bayesian approximation: Representing model uncertainty in deep learning. Preprint at <https://arxiv.org/abs/1506.02142> (2016).
38. Kendall, A. & Gal, Y. What uncertainties do we need in bayesian deep learning for computer vision? Preprint at <https://arxiv.org/abs/1703.04977> (2017).
39. Rives, A. *et al.* Biological structure and function emerge from scaling unsupervised learning to 250 million protein sequences. Preprint at <https://www.biorxiv.org/content/10.1101/622803v3> (2019).
40. Weininger, D. SMILES, a chemical language and information system. 1. introduction to methodology and encoding rules. *J. Chem. Inf. Comput. Sci.* **28**, 31–36 (1988).
41. Wu, Z. *et al.* MoleculeNet: a benchmark for molecular machine learning. *Chem. Sci.* **9**, 513–530 (2018).

42. Landrum, G. RDKit: Open-source cheminformatics. <http://rdkit.org> (2006).

43. Xie, T. & Grossman, J. C. Crystal graph convolutional neural networks for an accurate and interpretable prediction of material properties. *Phys. Rev. Lett.* **120**, 145301 (2018).

44. Kim, Q., Ko, J., Kim, S. & Jhe, W. GCIceNet: a graph convolutional network for accurate classification of water phases. *Phys. Chem. Chem. Phys.* **22**, 26340-26350 (2020).

45. Bapst, V. *et al.* Unveiling the predictive power of static structure in glassy systems. *Nat. Phys.* **16**, 448–454 (2020).

46. Battaglia, P., Pascanu, R., Lai, M., Rezende, D. J. & Kavukcuoglu, K. Interaction networks for learning about objects, relations and physics. *Adv. Neural Inf. Process. Syst.* 4502–4510 (2016).

47. Kwon, Y., Won, J.-H., Kim, B. J. & Paik, M. C. Uncertainty quantification using bayesian neural networks in classification: Application to ischemic stroke lesion segmentation. *Comput. Stat. & Data Analysis* **142**, 106816 (2020).

48. Paszke, A. *et al.* PyTorch: An imperative style, high-performance deep learning library. *Adv. Neural Inf. Process. Syst.* **32** 8024–8035 (2019).

49. Kingma, D. P. & Ba, J. Adam: A method for stochastic optimization. Preprint at <https://arxiv.org/abs/1412.6980> (2014).

Acknowledgements

This work was supported by the National Research Foundation of Korea (NRF) grant funded by the Korea Government (MSIP) (No. 2016R1A3B1908660).

Author contributions statement

All authors contributed to construct concept and initialize the project. Q.K and W.J made the program. All authors participated in the discussion of the results. Q.K and W.J wrote the manuscript. All authors reviewed the manuscript.

Competing interests

The authors declare no competing interests.

Table 1. ROC-AUC, Precision, and Recall scores of human and *C. elegans* dataset with proposed models, k-nearest neighbor (k-NN), random forest (RF), L2 logistic (L2), support vector machine (SVM), and graph neural network (GNN) proposed by Tsubaki *et al.*²². The best score of proposed models is emphasized in bold. The italicized scores correspond to the best scores for the baseline models.

Human

Methods	Balanced Dataset (1 : 1)			Unbalanced Dataset (1 : 3)		
	ROC-AUC	Precision	Recall	ROC-AUC	Precision	Recall
KNN	0.860	0.798	0.927	0.904	0.716	0.882
RF	0.940	0.861	0.897	<i>0.954</i>	0.847	0.824
L2	0.911	0.891	0.913	0.920	0.837	0.773
SVM	0.910	<i>0.966</i>	<i>0.950</i>	0.942	<i>0.969</i>	0.883
GNN	<i>0.970</i>	0.923	0.918	0.950	0.949	<i>0.913</i>
Trans6	0.968	0.902	0.901	0.971	0.915	0.910
Trans12	0.960	0.881	0.949	0.969	0.958	0.863
Trans34	0.973	0.914	0.925	0.971	0.930	0.863
Trans6+Drop	0.975	0.932	0.922	0.976	0.939	0.902
Trans12+Drop	0.971	0.914	0.924	0.963	0.932	0.902
Trans34+Drop	0.975	0.945	0.935	0.970	0.925	0.923

C. elegans

Methods	Balanced Dataset (1 : 1)			Unbalanced Dataset (1 : 3)		
	ROC-AUC	Precision	Recall	ROC-AUC	Precision	Recall
KNN	0.858	0.801	0.827	0.892	0.787	0.743
RF	0.902	0.821	0.844	0.926	0.836	0.705
L2	0.892	0.890	<i>0.877</i>	0.896	0.875	0.681
SVM	0.894	0.785	0.818	0.901	0.837	0.576
GNN	<i>0.978</i>	<i>0.938</i>	<i>0.929</i>	<i>0.971</i>	<i>0.916</i>	<i>0.921</i>
Trans6	0.981	0.937	0.949	0.977	0.871	0.917
Trans12	0.975	0.949	0.910	0.967	0.876	0.861
Trans34	0.973	0.914	0.925	0.969	0.900	0.915
Trans6+Drop	0.986	0.955	0.933	0.983	0.923	0.944
Trans12+Drop	0.980	0.946	0.928	0.981	0.890	0.940
Trans34+Drop	0.981	0.946	0.940	0.980	0.914	0.937

Table 2. Epistemic and aleatoric uncertainties for a range of different training dataset sizes (1, 1/2, 1/4 of the original training dataset size) The results show that the aleatoric uncertainty remains approximately constant, whereas the epistemic uncertainty increases when the training size decreases.

Dataset	Epistemic	Aleatoric
BindingDB / 4	0.018	0.036
BindingDB / 2	0.013	0.037
BindingDB	0.011	0.037
Human / 4	0.0128	0.020
Human / 2	0.0096	0.018
Human	0.0082	0.019
<i>C. elegans</i> / 4	0.0137	0.0155
<i>C. elegans</i> / 2	0.0098	0.0153
<i>C. elegans</i>	0.0053	0.0143

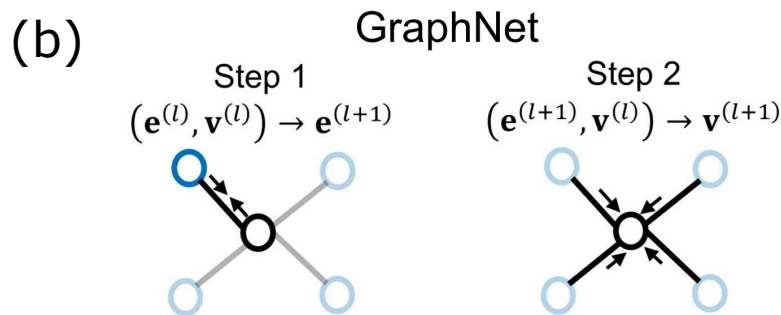
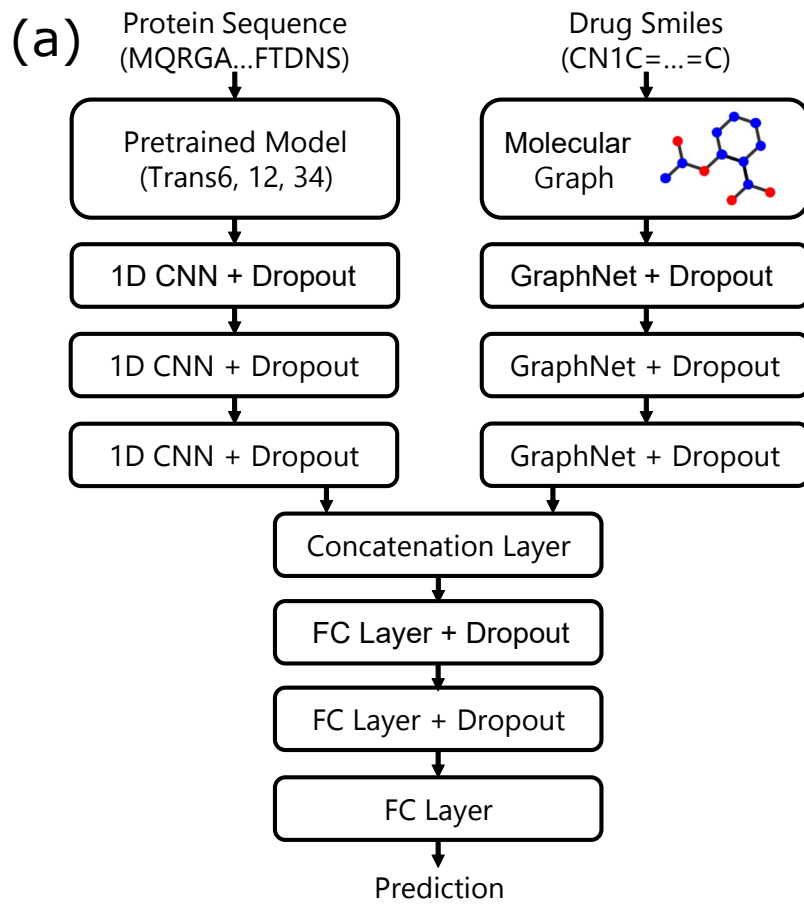


Figure 1. An overview of schematic of proposed neural network architecture. (a) The protein and drug representations are obtained by passing the pretrained transformer model and GraphNet layers, respectively. The protein and drug representation vectors are concatenated and fed into a classifier consisting of fully-connected layers. (b) Mechanism of the message passing in GraphNet. The GraphNet performs message passing on the molecular graph, recursively updating graph edges $\mathbf{e}^{(l)}$ and nodes $\mathbf{v}^{(l)}$.

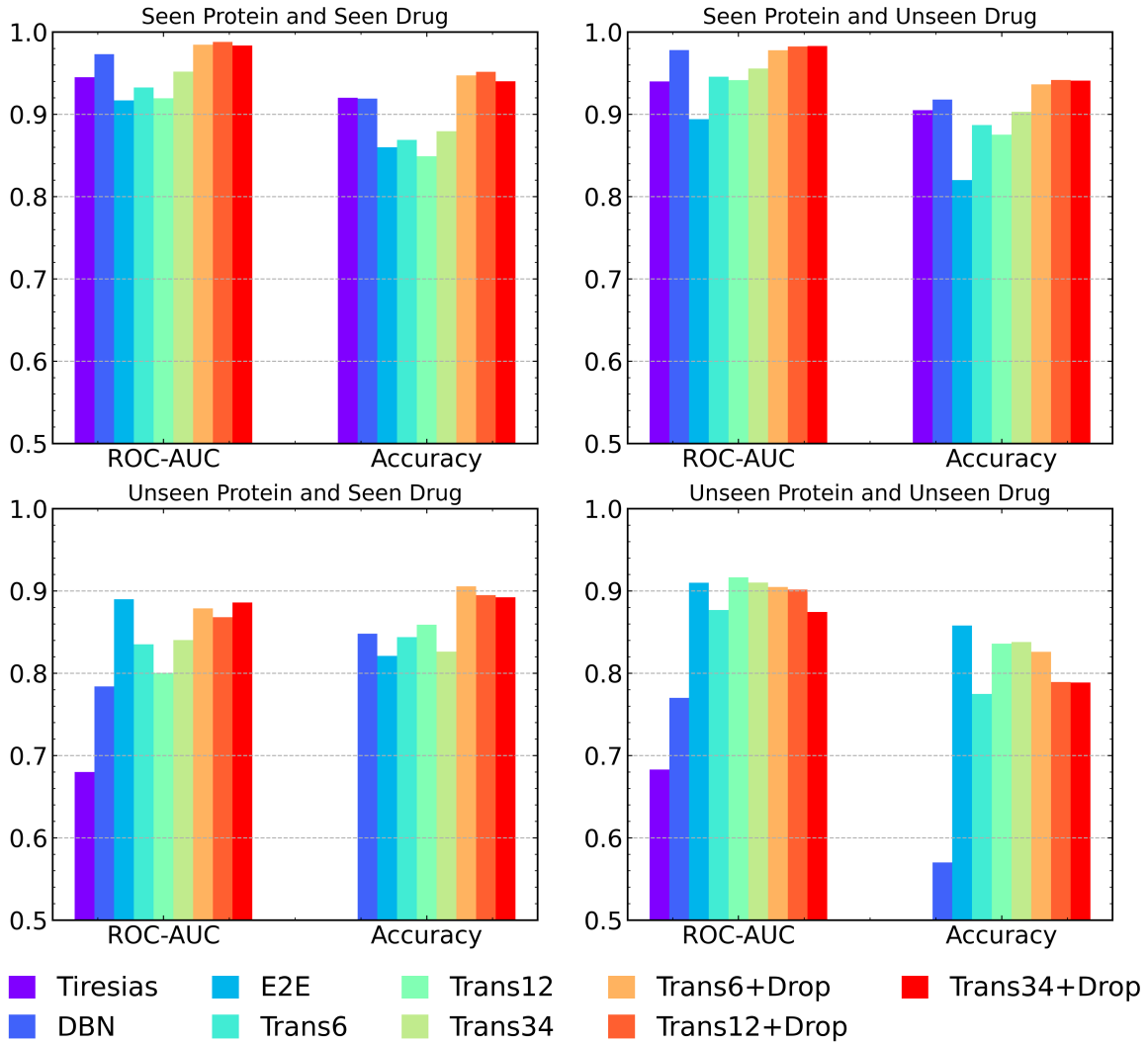


Figure 2. Performance comparison of proposed models, similarity-based approach (Tiresias), stacked restricted Boltzmann layers (DBN), and graph convolutional networks - long short-term memory-based approach (E2E). For each model, two metrics are reported: area under receiver operating characteristic curve (ROC-AUC) and accuracy. The binary interaction test data is divided by “seen” and “unseen” whether the protein and drug are observed in the training dataset. The accuracy score of Tiresias is not seen in the bottom graphs because they are lower than the lower bound of y -axis.

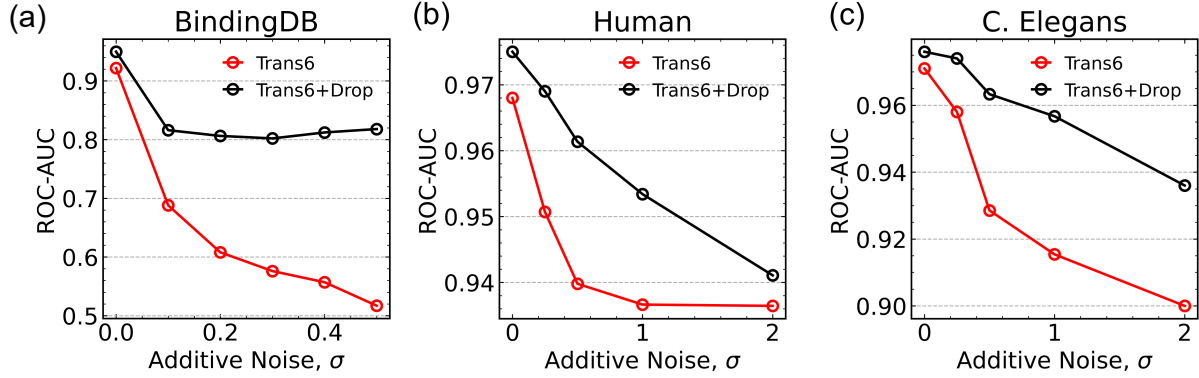


Figure 3. ROC-AUC scores on the test set as a function of standard deviation of the additive noise on (a) BindingDB, (b) Human, and (c) *C. Elegans* dataset. The additive noise is sampled from the Gaussian distribution $\mathcal{N}(0, \sigma^2)$.

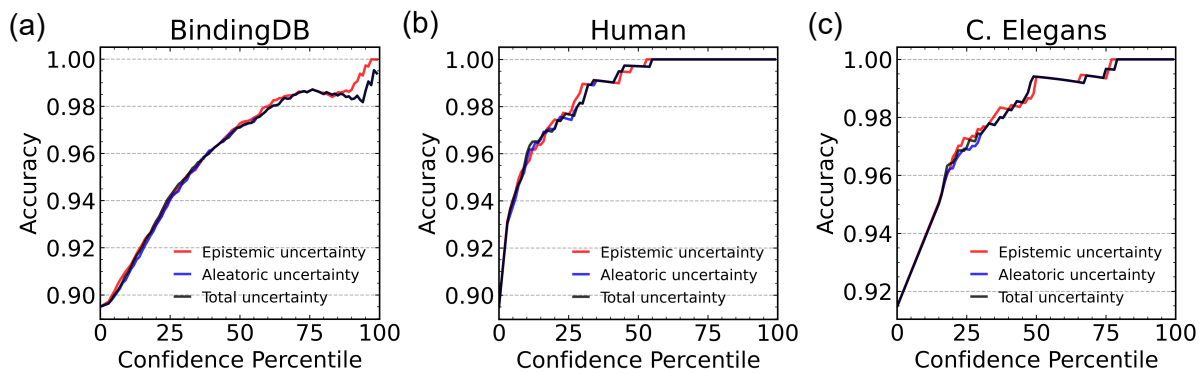


Figure 4. Model accuracies on the test set as a function of confidence percentile of (a) BindingDB, (b) Human, and (c) *C. Elegans* dataset. The confidence is estimated based on the epistemic uncertainty (red line), aleatoric uncertainty (blue line), and sum of the two (black line).